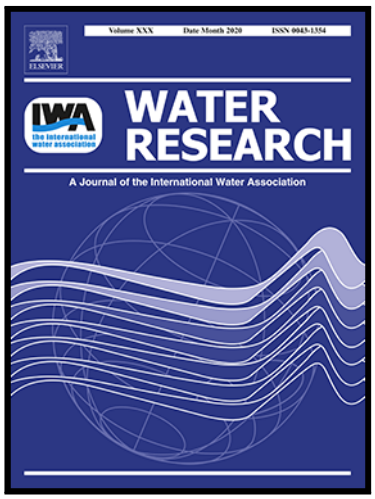

Density currents affect the vertical evolution of dissolved organic matter chemistry in a large tributary of the Three Gorges Reservoir during the water-level rising period

Kai Wang , Penghui Li , Chen He , Quan Shi , Ding He

PII: S0043-1354(21)00804-6
DOI: https://doi.org/10.1016/j.watres.2021.117609
Reference: WR 117609

To appear in: *Water Research*

Received date: 21 June 2021
Revised date: 20 August 2021
Accepted date: 23 August 2021

Please cite this article as: Kai Wang , Penghui Li , Chen He , Quan Shi , Ding He , Density currents affect the vertical evolution of dissolved organic matter chemistry in a large tributary of the Three Gorges Reservoir during the water-level rising period, *Water Research* (2021), doi: https://doi.org/10.1016/j.watres.2021.117609

Density currents affect the vertical evolution of dissolved organic matter chemistry in a large tributary of the Three Gorges Reservoir during the water-level rising period

Kai Wang[a,c], Penghui Li[d,f], Chen He[e], Quan Shi[e], Ding He[b,a,*] dinghe@zju.edu.cn

[a]Organic Geochemistry Unit, School of Earth Sciences, Zhejiang University, Hangzhou 310027, China

[b]Department of Ocean Science, The Hong Kong University of Science and Technology, Hong Kong 999077, China

[c]State Key Laboratory of Hydro-science and Engineering, Department of Hydraulic Engineering, Tsinghua University, Beijing 100084, China

[d]School of Marine Sciences, Sun Yat-sen University, Zhuhai 519082, China

[e]State Key Laboratory of Heavy Oil Processing, China University of Petroleum, Changping District, Beijing 102249, China

[f]Southern Marine Science and Engineering Guangdong Laboratory (Zhuhai), Zhuhai 519082, China

[*]Corresponding Author.

Highlights

- Various DOM sources in surface, middle, and bottom were investigated in XXB.
- Property variations of DOM in water column were affected by reservoir construction-induced density current.
- Vertical variations of DOM could affect CO_2 emission and carbon burial in reservoirs

Graphical Abstract

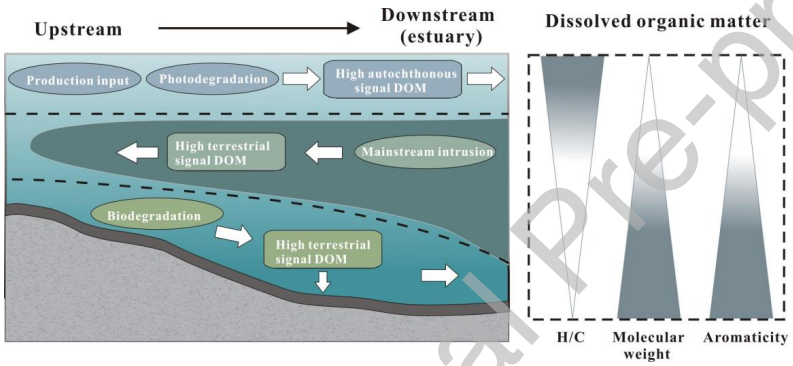

Abstract

Reservoirs have boomed for clean energy in recent decades and interrupted the natural river ecosystem severely. Riverine dissolved organic matter (DOM), which regulates aquatic food web dynamics, water quality, and carbon storage, has been significantly impacted by reservoir construction. However, the vertical evolution of DOM properties and its controlling mechanisms in large reservoirs with hydrological management are not well investigated, limiting the understanding of carbon cycling (e.g., CO_2 emissions and carbon burial) in reservoirs. To fill this knowledge gap, multiple complementary techniques including optical spectroscopy and

ultrahigh-resolution Fourier transform ion cyclotron resonance mass spectrometry were applied to track composition and property changes of DOM along the vertical profile in a large deep tributary of the world largest Three Gorges Reservoir (TGR) during the water-level rising period. The results indicated that middle and bottom water have relatively more terrestrial input and recalcitrant DOM, while surface water has relatively more autochthonous input and labile DOM. Integrated with the comprehensive analysis of DOM chemistry in a high-resolution vertical profile, the primary production and photodegradation in surface water, the density currents induced water intrusion from mainstream to tributaries, in middle water, and the biodegradation in bottom water are main factors controlling the vertical heterogeneity of reservoir DOM during the water-level rising period. This vertical increase of DOM recalcitrance likely contributes to the enhancement of organic carbon burial in TGR during the water-level rising period. All in all, this study provides new insight into the vertical variations of riverine DOM induced by reservoir construction, and emphasizes the important role of reservoir construction in carbon sequestration.

Keywords

Dissolved organic matter; vertical heterogeneity; FT-ICR MS; Three Gorges Reservoir

1. Introduction

Considering rivers play a crucial role in the linkage between the land and sea, the dynamics of riverine dissolved organic matter (DOM), the complex mixture of organic compounds with different reactivity, has exerted a significant influence on the carbon connection between terrestrial and oceanic ecosystems (Raymond and Bauer, 2001; Jaffé et al., 2012; Mendonça et al., 2016, 2017). The transport and transformation of DOM in the water column consist an important part of carbon cycling, which links both CO_2 emissions to the atmosphere and organic carbon burial in sediments of aquatic ecosystems. Previous studies illustrated that DOM

transported from surface to bottom with humic-like component increased and recalcitrant dissolved organic carbon (DOC) enriched, and involved in carbon mineralization (greenhouse gas emission) and fixation (carbon burial) processes (Lee and Wakeham, 1992; Arstegui et al., 2002; Cory et al., 2015; Bergauer et al., 2018). Thus, clarifying the mechanism of riverine DOM variation in the water column is crucial for a better understanding of carbon cycling. Geological factors (e.g., regional watershed heterogeneity) functioned in DOM dynamics (e.g., photodegradation and biodegradation) through altering light or microorganism context have been revealed (Cory et al, 2015). Besides, hydrology has been increasingly acknowledged to influence the heterogeneity of DOM significantly (Miller et al., 2009; D. He et al., 2020; She et al., 2021).

Natural hydrologic variations (e.g., changes in water level and discharge) did exert an impact on the composition and reactivity of DOM in water columns through altering water residence time and structure (Stubbins et al, 2010; Cory et al., 2014). For instance, in natural lakes and oceanic settings, water stratification or external water mass intrusion would influence water structure and could isolate surface water from middle or bottom water, leading to high variations in quantity (e.g., concentrations decreasing of organic carbon) and quality (e.g., terrestrial humic-like signature) of DOM along the surface to bottom water column (Gareis et al., 2010; Cory et al, 2015; Medeiros et al., 2015; She et al., 2021). In contrast to natural aquatic ecosystems, reservoirs are one of the most far-reaching human modifications of hydrological conditions of rivers and have a complicated water stratification regime due to hydrological management (Maavara et al., 2020). Compared with the investigation of nutrients, and quantity of organic and inorganic carbon, whether the hydrological management will affect the vertical characteristics (i.e., from surface to bottom) of DOM chemistry is poorly understood (Yi et al., 2021), which is particularly important considering the bottom drainage strategy of reservoirs (reservoir water was drained from dam bottom to downstream) (Maavara et al., 2020). Reservoir construction has been proved to affect the light conditions, hydraulic retention time, and relative water column stability (RWCS), resulting in different degrees of change in the transport and transformation of materials (e.g., nutrients) in different layers of the water column, especially in deep tributaries with longer water retention time than the mainstream of reservoirs (Burford et al., 2012; Wang, 2020). However,

systematic research on how reservoirs alter riverine DOM chemistry in water columns remains lacking.

Three Gorges Reservoir (TGR), the largest artificial reservoir in the world, has influenced the ecosystem of the Yangtze River watershed significantly, with a storage capacity of 39.3 billion m^3 and a watershed area of 1080 km^2. With reservoir operation, a semi-lake/semi-river system has been formed (e.g., D. He et al., 2020). The hydrological management-induced variations in the flow speed, water level, and water structure, which complex the regimes of water residence, nutrient retention, and sediment trapping (Hu et al., 2013; Dai et al., 2013; Yang et al., 2018). In particular, the increase of water residence time amplifies primary productivity in surface water and reduces the proportion of photic zone in vertical profile, which would enhance the biogeochemical heterogeneity in the water column (Yang et al., 2019; Zhang et al., 2019; Chen et al., 2020). However, it is still mysterious whether the TGR construction makes a significant impact on the vertical variation of DOM in water columns, and further on the biogeochemical and carbon cycles in reservoirs.

For the investigation of the complex composition of DOM, multiple complementary methods including optical and molecular techniques have been developed. Ultraviolet-visible (UV-Vis) absorption and the fluorescence excitation-emission matrix (EEMs) technique with parallel factor analysis (EEM-PARAFAC) have been widely applied to depict the characteristics of DOM in aquatic ecosystems (Jaffé et al., 2008; Huguet et al., 2009). In recent decades, Fourier transform ion cyclotron resonance mass spectrometry (FT-ICR MS) has been increasingly applied to track the sources of DOM at the molecular level (Kujawinski et al., 2002; Melendez-Perez et al., 2016; Wang et al., 2019, 2021a). The combination of the optical properties and molecular composition of DOM could help to better qualitatively and quantitatively constrain its biogeochemical behaviors, and provide a comprehensive understanding from the bulk to the molecular level (Stubbins et al., 2014; Lavonen et al., 2015).

We selected Xiangxi Bay (XXB) to investigate the DOM chemistry in water columns. XXB is a large deep (depth > 50m) tributary of TGR. In addition, it is closest to the Three Gorges Dam, and previous studies have successfully constrained its hydrologic model (Ji et al., 2010; Yang et al., 2018). Therefore, XXB could provide a typical case for investigating how reservoir construction would affect the vertical evolution of DOM chemistry. In terms of the sampling strategy, in addition

to spatial sampling in surface, middle, and bottom layers of multiple sites, which provides good coverage to constrain the DOM sources across XXB, we targeted a series of high-resolution water column samples from a site with the deepest water depth to monitor DOM vertical variations and explore the underlying mechanisms. Through the application of a series of approaches including bulk geochemical techniques, UV-Vis, EEMs, and FT-ICR MS, the objectives were to i) characterize the property variation of DOM in vertical profiles of XXB, ii) determine the role of reservoir construction in shaping the vertical heterogeneity of DOM, iii) explore the linkage between vertical heterogeneity of DOM and carbon cycling (e.g., CO_2 emission and carbon burial) in the TGR.

2. Materials and methods

2.1. Site description

XXB is a large and deep tributary of the Yangtze River covered by the TGR backwater. It is located between Jingshan and Wushan Mountains and originates from the Shennongjia National Forest Park which is at a distance of 123 km from the Three Gorges Dam (TGD) (Fig. 1a). The watershed of XXB has a subtropical monsoon humid climate (average annual temperature: 18.9 ℃; annual precipitation: 1023 mm).

2.2. Sample collection

We designed 11 sampling sites (XX00 to XX10) to investigate the variability of DOM properties in XXB (Fig. 1). Surface (sampled at approximately 1 m below the surface), middle (sampled at about half of the water depth), and bottom (sampled at about 5 m above the bottom) water samples were collected at each site from XX00 to XX10 (n=33). In addition, a series of high-resolution water column samples (depths of 2m, 5m, 10m, 15m, 20m, 30m, 40m, 50m, 60m) (n=9) was collected at XX00 (Fig. 1b, c). Surface and bottom samples were also collected in mainstream sampling sites (M01, M02, and M03) (n=6). The sampling was carried out during the water-level rising period of TGR (October 20th, 2018).

All water samples were collected using hydrochloric acid (trace metal) precleaned Nalgene bottles, transported to the lab on ice. Water samples were filtered

through precombusted 0.7 μm glass fiber filters (Whatman GFF) and 0.22 μm membrane filters (Millipore) to remove particles, algal aggregates, and most bacteria within 24 hr of sampling to obtain DOM in water (Wang et al., 2021a).

2.3. Bulk characteristic analyses

Water temperature, dissolved oxygen (DO), turbidity, pH, and chlorophyll-a (Chla) were measured using a calibrated multiprobe (EXO2; YSI, USA). Relative water column stability (RWCS), the parameter used to depict the stratification conditions (Padisák et al., 2003), was calculated following Eq. (1):

$$\mathrm{RWCS} = \frac{\rho_b - \rho_w}{\rho_4 - \rho_5} \quad (1)$$

Where ρ_b and ρ_w represent the bottom water density and water density at a certain depth, respectively, and ρ_4 and ρ_5 represent the water density at 4℃ and 5℃, respectively.

The water density was calculated from Eq. (2) based on the value of temperature (T) (Martin and McCutcheon, 1998; Lawson and Anderson, 2007):

$$\rho = 1000 * 1 - \left[1 - \frac{T+288.9414}{508929.2*(T+68.1296)} * (T - 3.9863)^2\right] \quad (2)$$

5 ml of 0.22 μm-filtered water sample was quantified for concentrations of ions including K^+, Mg^{2+}, and Ca^{2+}, by Dionex ICS-3000. 20 mL of 0.22 μm-filtered samples were acidified to pH = 2 to remove any inorganic carbon and then quantified for dissolved organic carbon (DOC) by high-temperature catalytic oxidation (TOC-L analyzer, Shimadzu) (< 2%, coefficient of variation).

2.4. Optical and molecular analysis of DOM

Optical analysis including UV-Visible absorbance and 3D-EEM were conducted on Aqualog (Horiba, Japan) absorption-fluorescence spectrometer, during which Raman scattering and Inner-filter effects were calibrated (Li et al., 2015). Slope ratio (S_R, proxy for DOM molecular weight), aromatic index [$SUVA_{254}$ (L mg-C^{-1} m^{-}

[1])], fluorescence index (FI), humification index (HIX), and biological index (BIX) were calculated based on spectroscopic analysis (Hansen et al., 2016 and reference therein). Parallel factor analysis (PARAFAC) was also carried out based on 3D-EEM (Stedmon and Bro, 2008).

1L 0.22 μm-filtered and acidified (pH=2) samples were extracted by solid-phase extraction (SPE) using 500 mg Agilent Bond Elut PPL cartridges and eluted by 4 ml methanol to pre-combusted glass ampoules after the dry of ultra-high purity nitrogen gas (Dittmar et al., 2008). Eluted methanol samples would be stored in dark at -20 °C before analysis. The recovery efficiencies of Agilent Bond Elut PPL (the ratio of extracted organic carbon in methanol eluent to original organic carbon in water sample) ranged from 50% to 60%. Methanol eluent of SPE-DOM (DOM extracted by solid-phase extraction) was analyzed with a 9.4 T Apex-ultra X FT-ICR MS (the Heavy Oil Key Laboratory, China University of Petroleum) under negative mode (128 scans) with an electrospray ionization source (Bruker Apollo II) (C. He et al., 2020). Formulas (CHO, CHON, CHOS, and CHONS classes; $C_{\leq 60}$, $H_{\leq 120}$, $O_{\leq 30}$, $N_{\leq 3}$, $S_{\leq 1}$) ranged from 200 to 850 Da, were assigned to peaks with signal-to-noise ratio >4 and a detection error <1 ppm of absolute mass. A semi-quantitative assessment of the molecular formula was carried out based on the relative peak intensities (normalized to all molecular peak intensities per sample). Elements (C, H, O, N, S), H/C, O/C, formular classes (CHO, CHON, CHOS, CHONS), double bond equivalent (DBE), modified aromaticity index (AI) were obtained (D. He et al., 2020). To provide more comprehensive information on DOM composition, various molecular groups attributed to different sources were categorized as: polycyclic aromatics (PCAs, $AI \geq 0.67$), polyphenols ($0.66 \geq AI \geq 0.50$), highly unsaturated compounds, which include soil-derived products of lignin degradation ($AI < 0.50$, $H/C < 1.5$), unsaturated aliphatic compounds ($2.0 \geq H/C > 1.5$, $N = 0$), and peptides ($2.0 > H/C \geq 1.5$, $N > 0$). The molecular lability index (MLB_L), an indicator to evaluate the overall lability of DOM (D'Andrilli et al., 2015), was calculated. Besides, the carboxyl-rich alicyclic molecules (CRAMs), which are a major component of the refractory organic matter, are also identified (Hertkorn et al., 2006).

2.5. Statistical analyses

To assess the difference of DOM in different layers (surface, middle, and bottom), the Student t-test was conducted on R3.2.1 (R Core Team 2015) to verify the

differences among bulk, optical, and molecular parameters (DOC, HIX, $SUVA_{254}$, O/C, H/C, DBE, AI, m/z, polyphenols%, highly unsaturated compounds%, peptides%, and unsaturated aliphatics%). The Pearson correlation analysis was applied to investigate the vertical variation trend of DOM optical and molecular parameters. To demonstrate the variation of DOM, a principal component analysis (PCA) was also conducted to select from the bulk, optical, and molecular parameters (HIX, $SUVA_{254}$, O/C, and H/C, etc.).

3. Results

3.1. Bulk and optical properties of DOM

The average DOC concentration was higher in surface water (1.25 ± 0.04 mg/L) than in middle (1.08 ± 0.04 mg/L) and bottom water (1.13 ± 0.06 mg/L), while was similar between middle and bottom water (Fig. 2a).

The average values of HIX and $SUVA_{254}$ were all lower in surface water (HIX: 0.59 ± 0.02; $SUVA_{254}$: 4.00 ± 0.22 L mg-C^{-1} m^{-1}) than in middle (HIX: 0.65 ± 0.02; $SUVA_{254}$: 4.89 ± 0.18 L mg-C^{-1} m^{-1}) and bottom water (HIX: 0.64 ± 0.02; $SUVA_{254}$: 4.44 ± 0.28 L mg-C^{-1} m^{-1}) (Fig. 2b, S1b; Table S1), while FI, BIX, and S_R were all higher in surface water (FI: 1.74 ± 0.02; BIX: 0.89 ± 0.01; S_R: 1.59 ± 0.08) than in middle (FI: 1.69 ± 0.01; BIX: 0.84 ± 0.01; S_R: 1.21 ± 0.04) and bottom water (FI: 1.71 ± 0.01; BIX: 0.85 ± 0.01; S_R: 1.13 ± 0.05) (Fig. 2c, S2a, c; Table S1). There were similar HIX, $SUVA_{254}$, FI, BIX, and S_R values in middle and bottom water. All optical parameters showed no significant trends along spatial transects from upstream (XX10) to downstream (XX00) for surface, middle, and bottom water samples, respectively.

Two humic-like fluorescent components (C1 and C3) and two protein-like fluorescent components (C2 and C4) were obtained through the EEM-PARAFAC analysis (Fig. S3). Components C1 and C3 were usually characterized as terrestrial humic-like DOM from farmland environments, while components C2 and C4 were usually recognized as tryptophan-like component and tyrosine-like component, respectively (Table S2) (Stedmon et al., 2005; Murphy et al., 2006, 2011, 2014; Osburn

et al., 2011, 2016; Yamashita et al., 2011; Cawley et al., 2012; Graeber et al., 2012). The average relative proportions of C1 and C3 components showed lower values in surface water (45 ± 2%) than those in middle (51 ± 2%) and bottom water (48 ± 2%) (Fig. 2d), whereas the average relative proportions of C2 and C4 components showed the opposite variations (Fig. 2e). C1, C2, C3, and C4 showed no significant variations along spatial transects from upstream to downstream for surface, middle, and bottom water samples, respectively.

3.2. Molecular composition of SPE-DOM determined by FT-ICR MS

A total of 13260 unique formulas (CHO: 5225; CHON: 4227; CHOS: 3086; CHONS: 722) were identified by FT-ICR MS (Fig. S4). 11661 (CHO: 4617; CHON: 3743; CHOS: 2694; CHONS: 607), 11061 (CHO: 4533; CHON: 3441; CHOS: 2600; CHONS: 487), and 10757 (CHO: 4656; CHON: 3483; CHOS: 2223; CHONS: 505) unique formulas were identified in surface, middle, and bottom water samples (Table S3), respectively, while 9181 (CHO: 4063; CHON: 2945; CHOS: 1788; CHONS: 385) formulas were co-occurred (present in all samples; Fig. S4). The average relative abundance of CHO compounds was lower in surface water (65.86 ± 2.38%) than in middle (70.71 ± 2.09%) and bottom water (72.16 ± 1.58%), whereas the average relative abundance of heteroatomic compounds (e.g., CHON and CHOS) varied oppositely (Fig. S5; Table S4). CHO and heteroatomic compounds varied little between middle and bottom waters (Fig. S5; Table S4).

In terms of molecular parameters derived from FT-ICR MS, m/z, AI, and DBE showed lower values in surface water (m/z: 446.71 ± 3.37; AI: 0.25 ± 0.01; DBE: 9.31 ± 0.09) than in middle (m/z: 455.71 ± 2.53; AI: 0.26 ± 0.01; DBE: 9.68 ± 0.09) and bottom water (m/z: 455.89 ± 2.78; AI: 0.26 ± 0.01; DBE: 9.77 ± 0.07) (Fig. 2f, g; Fig. S2c, d), while MLB_L showed higher values in surface water (13.32 ± 0.46) than in middle (11.28 ± 0.57) and bottom water (10.98 ± 0.45) (Fig. S2e). Concerning the molecular groups, there were lower average relative abundances of more aromatic (biologically recalcitrant) compounds (polyphenols and highly unsaturated compounds) in surface water (89.22 ± 1.03%) than in middle (92.64 ± 0.73%) and bottom water (93.08 ± 0.60%), whereas higher averaged relative abundances of more aliphatic (biologically labile) compounds (unsaturated aliphatic compounds and peptides) in surface water (9.66 ± 0.98%) than in middle (6.38 ±

0.58%) and bottom water (6.08 ± 0.53%) (Fig. 2h, i; Table S5). Both molecular parameters (e.g., m/z, DBE, and AI) and groups (e.g., polyphenols, highly unsaturated compounds, unsaturated aliphatic compounds, and peptides) showed no significant variations between middle and bottom water samples (Fig. 2, S2).

3.3. Principal component analysis based on optical and molecular information

Principal component analysis was carried out based on optical and molecular analyses (Fig. S6). The loadings of the first and second principal components (PC1 and PC2) explained 58% and 17% of the variations of DOM alteration (Fig. S6). Parameters associated with molecular humification and aromaticity (e.g., AI, and DBE) are located on the positive loadings of PC1, while parameters associated with freshly produced and biologically labile DOM (e.g., UA+Peptides and MLB_L) are located on the negative loadings of PC1. Optical parameters tend to be mainly associated with PC2. Humification and aromaticity associated optical parameters (e.g., HIX and $SUVA_{254}$) are located on the positive loadings of PC2, while C2+C4 is located on the negative loadings of PC2. The surface samples were separated from middle and bottom samples mainly based on PC1, which indicated that there were likely larger variations in molecular properties than in optical properties.

3.4. The variation of bulk characteristics and DOM chemistry along a high-resolution vertical profile

There were significant physicochemical gradients along the vertical profile, which divided the water column into three layers: surface (0-5m), middle (5-30m), and bottom (30-60m) (Fig. 3). There were significant decreasing trends of Chla, DO, Turbidity, pH, and RWCS with depth (from surface to bottom and middle to bottom; Fig. 3).

The vertical profile showed a significant decrease of DOC concentration from surface to bottom water ($p < 0.01$) (Fig, 5a). In terms of optical properties, HIX and C1+C3 (%) increased from surface to bottom water, while BIX and C2+C4 (%) decreased (Fig. 4b, c, d, e). FT-ICR MS analysis exhibited that O/C, m/z, AI, DBE significantly increased from surface to bottom, while H/C decreased (Fig. 4f, g, h, i, j). In terms of composition, the relative percentages of CHON and CHOS compounds significantly decreased from surface to bottom, whereas the relative percentage of CHO compounds showed the opposite trend (Fig. 4k, l, m). HU+Poly

significantly increased but UA+Peptides significantly decreased from surface to bottom (Fig. 4n, o).

4. Discussions

4.1 Sources identification of DOM in XXB

The material sources of inland water (e.g., primary productivity, riparian soil, and sewage) constrain the various possible DOM sources in aquatic ecosystems (e.g., autochthonous, terrestrial, and anthropogenic sources) (Amon et al., 2012). Optical parameters preliminarily demonstrated the multiple sources of DOM in XXB. The range of FI (1.58 to 1.80), which has been widely used to classify DOM sources with FI values of >1.9 as autochthonous (microbial or algae-derived), with FI values of <1.4 as allochthonous (terrestrially derived), and with FI values of 1.4 to 1.9 as mixed sources, suggested both allochthonous and autochthonous inputs of DOM in TGR (Table S2) (Fellman et al., 2010). The values of $SUVA_{254}$ (3.01 ~ 6.35 L mg-C^{-1} m^{-1}) and HIX (0.48 ~ 0.79) also indicated that DOM was derived from sources with a wide range of aromaticity and humification degree (Table S2) (Ohno et al., 2007). In terms of molecular information, the wide range of AI (0.22 ~ 0.28) and DBE (8.78 ~ 10.12) values, which were used to assess the aromaticity and unsaturation degree, further confirmed the multiple sources of DOM (Table S4) (Dittmar et al., 2008).

Two humic-like components (C1 and C3), which are widely found in lakes and estuaries, have been proved to derive from terrestrial input (Table S2) (Stedmon et al., 2005; Murphy et al., 2014). Furthermore, the detection of polyphenols and highly unsaturated compounds by FT-ICR MS, which were mainly related to vascular-plant-sourced organic matter and products of lignin degradation, respectively, also demonstrated the input of terrestrial organic matter (Seidel et al., 2015). In terms of autochthonous input, Osburn et al. (2016) have identified similar components with C4 and suggested that this component was associated with aquatic organisms' production. The detection of peptides and unsaturated aliphatics by FT-ICR MS indicated that bacterial and algal-derived OM contributed to DOM in TGR as well (Table S6) (Seidel et al., 2015; Kellerman et al., 2018). The protein-like component C2 shared the similar EEMs peak region with wastewater-sourced component C5

reported by Murphy et al. (2014) and Cawley et al. (2012) and indicated the anthropogenic input (Table S2). From the FT-ICR MS, a series of CHOS compounds with O_3S and O_5S classes were detected, which were previously detected as an indicator of anthropogenic input in anthropogenically perturbated waters including wastewater and associated with surfactants (Table S4, S7) (Gonsior et al., 2011; Melendez-Perez et al., 2016; Wang et al., 2019).

4.2 Transformation of DOM along the vertical profile and the controlling mechanism

Optical and molecular properties preliminarily exhibited variations of DOM chemistry with water depth. There was a higher proportion of terrestrial-derived DOM, and a lower proportion of autochthonous and anthropogenic-derived DOM in middle and bottom water compared to surface water (Fig. 2 and S2), which was also supported by the principal component analysis (Fig. S6). Moreover, the continuous evolution of DOM chemistry was further assessed through the analysis of high-resolution samples along the vertical profile. The decreasing trends of BIX, C2+C4, H/C, UA+Peptides, and increasing trends of HIX, C1+C3, O/C, m/z, AI, DBE, HU+Poly demonstrated that the aromaticity, humification degree, molecular weight, and proportion of terrestrial sourced DOM increased with water depth from 2m to 60m, whereas the proportion of autochthonous sourced DOM decreased (Fig. 4; Table S8).

Various studies have proved the strong linkage between hydrology and DOM chemistry (D. He et al., 2020; Wang et al., 2021a). The hydrological model in XXB has been well established by Ji et al. (2010), which exhibited that the density current associated with water intrusion from mainstream to the tributary, mainly induced the water stratification (Fig. 2a). Since the water in the mainstream is characterized by higher concentrations of K^+ and Ca^{2+}, the concentration variations of K^+ and Ca^{2+} (significant increasing trends from upstream to downstream for the middle and bottom water layers), further confirm this hydrological model (Fig. 2b, c, d, e) (Yang et al., 2015). In addition, no significant trends of concentrations of K^+ and Ca^{2+} were observed for the surface water layer, indicating that the water intrusion from mainstream to XXB was mainly constrained in the middle and bottom layers. Therefore, integrated with the constrained water exchange model, a conceptual model of DOM dynamics was established to account for the vertical variations of DOM chemistry in the water column (Fig. 5).

In the surface water layer (0 ~ 5m), the high primary productivity indicated by high concentrations of Chla would devote to the enrichment of peptides and unsaturated aliphatics including $CHON_2$, $CHON_3$, CHOS compounds with high H/C (e.g., $C_{15}H_{16}O_{11}N_2$, $C_{35}H_{39}O_{12}N_3$, $C_{16}H_{24}O_7S_1$) (Henderson et al., 2008; Zhou et al., 2014; Ly et al., 2017; He et al., 2019). The depleted CHO compounds with low O/C were possibly associated with selective photodegradation of aromatic compounds (Stubbins et al., 2010; Chen et al., 2014; D. He et al., 2020). This is further supported by the detection of photodegradation produced compounds (with high averaged H/C but low AI, m/z, and DBE; Table S9; Fig. S7a) through comparison between surface formulas and photodegradation produced DOM pool, which was identified by the incubation experiment from our previous study (Wang et al., 2021b) (Supplementary method 1.7; Table S10). Therefore, high autochthonous derived DOM with low aromaticity, humification degree, and molecular weight was exhibited in the surface layer (Fig. 4).

In the middle water layer (5 ~ 30m), the reservoir operation induced density current drove mainstream water intrusion to XXB (Fig. 2a). Since the mainstream DOM had a high terrestrial signal (Table S11), it increased the terrestrial signature of the middle water layer samples in XXB. In addition, polyphenols and highly unsaturated compounds including CHO compounds with high O/C, humification degree and aromaticity could be accumulated and enriched in middle layer water due to limited illumination-induced photodegradation (sunlit layer < 5m, Stubbins et al., 2010; He et al., 2018).

Compared with the surface and middle layers, previous studies have demonstrated that microbial carbon pump (MCP) functioned in deep water through biodegradation and devote to the long-term accumulation of recalcitrant DOM (Findlay et al., 2003; Jiao et al., 2010; Yi et al., 2021). Correspondingly, the relatively lower averaged concentration of DO than surface water and decrease of DO with depth (30 ~ 60m) support further OC mineralization in the bottom layer (Fig. 3b). Therefore, the high terrestrial signal of DOM in bottom water might mainly result from biodegradation (Medeiros et al., 2015), which agreed with the high relative abundance of biologically recalcitrant compounds including polyphenols and highly unsaturated compounds. Besides, the identification of various CRAMs and biodegradation produced compounds (with low H/C, high m/z, DBE, and AI; Table S9; Fig. S7b) through comparison between bottom formulas and biodegradation

produced DOM pool suggest active microbial carbon pump which also supported this point (Wang et al., 2021b) (Supplementary method 1.7; Table S10). Also, the accumulation of terrestrial DOM from the middle layer would partly devote to the high terrestrial signal of DOM in bottom water.

Previous studies have demonstrated that the variation of DOM in the water column would be affected by a regime of water stratification (Loginova et al., 2016; Butturini et al., 2020; Yi et al., 2021). In this work, the linkage between DOM chemistry and reservoir management induced RWCS, the parameter applied to assess the degree of water stratification, was confirmed by significant correlations between DOM molecular composition (i.e., various molecular parameters) and RWCS (Fig. S8). Therefore, the vertical heterogeneity of DOM in the water column is shaped by reservoir construction. which is likely a typical phenomenon present in multiple tributaries considering the widely observed density currents from the mainstream to tributaries of TGR (Yang et al., 2018).

4.3 Implications for carbon cycling and further considerations

With the multiple bulk and molecular level techniques, the dynamic process of DOM in the vertical profile of TGR was illustrated (Fig. 5), which was different from other aquatic ecosystems. For instance, the m/z and AI of DOM from surface to bottom layers of TGR here spanned wider ranges than those in lakes (e.g., Butturini et al., 2020; m/z: 354.4~365.0 Da, AI: 0.19~0.23). The composition structure (e.g., the abundance of CHO, CHON, CHOS compounds) of DOM from surface to bottom varied oppositely with those observed in the ocean (Medeiros et al., 2015). To assess this reservoir construction interrupted vertical dynamic of DOM comprehensively, the molecular comparison of DOM quality in the water column between reservoirs and other natural aquatic ecosystems (e.g., rivers and lakes) was further evaluated based on DBE and m/z (Fig. 6). A significant positive correlation between DBE and m/z was observed across reservoir, river and lake ecosystems (Fig. 6). Interestingly, the cluster of DOM in the water column of TGR was separated from others for the higher m/z and DBE values than in rivers and lakes, indicating that the operation of TGR not only induced unique DOM stratification but also shaped molecular composition into more unsaturation and recalcitrance, and higher averaged molecular weight (Hansen et al., 2016), which might be attributed to the variations in sources and transformation due to density currents and MCP due to reservoir construction

induced water depth increasing (Jiao et al., 2010).

As the major form of reactive carbon, DOM played an important role in regional carbon cycling (Stedmon et al., 2003). The reservoir construction induced vertical heterogeneity of DOM thus exerts a non-negligible influence on carbon processes. The isolation of surface water from middle and bottom water results from density current decreases the material connection between surface and bottom (Fig. 2a) (Yang et al., 2018). Thus, the primary productivity-related DOM (e.g., alga-derived protein-like compounds) would be partially retained in surface water and drained downstream instead of depositing to the bottom. Since the deposition of organic matter in the surface water column would increase microbial activities in middle and bottom layers (e.g., biodegradation) (Jiao et al., 2010), the interruption of vertical mixing would likely exclude surface DOM from biodegradation in middle and bottom water and devote to the reduction of microbial activity-related CO_2 production in the tributary. Moreover, the addition of biodegradation-resistant terrestrial DOM would dilute the proportion of autochthonous DOM in middle and bottom water which tends to be the substrate for heterotrophic microorganisms, and reduce biodegradation-related CO_2 production (Saadi et al., 2006; Hansen et al., 2016). Most of the terrestrial DOM compounds brought by density current in the water column are aromatic with high molecular weight and environmental stability, and tend to be well reserved in the water column (Catalán et al., 2017). By adsorbing on particulate matter and flocculation with metal ions, terrestrial DOM compounds including C1 and C3 associated compounds, polyphenols and highly unsaturated compounds would devote to the accumulation of organic matter in water columns and sediments, making a critical contribution to OC burial (Schmidt et al., 2009; Jacinthe et al., 2012). Reservoir construction has been proved to interrupt the carbon delivery of rivers (250-260 Tg C yr^{-1}) from land to ocean by a significant in situ carbon burial (26 Tg C yr^{-1}) with a complicated and unclarified mechanism (Maavara et al., 2017). Our observed vertical evolution of DOM chemistry would devote to a better understanding of the carbon burial mechanism in reservoirs.

Some limitations still exist in this study. Firstly, this research was conducted during the water-level rising period of TGR, a seasonal investigation, including the water-level falling period, highest and lowest water level periods, of DOM variation in the vertical profile is needed to better clarify the vertical dynamic of DOM

chemistry. Secondly, particulate organic carbon (POC) also relates to OC burial in reservoirs, but it is not constrained in this study. Although POC is usually characterized by significantly lower concentrations than DOC in most inland waters, the linkage between DOC and POC, and its contribution to the OC in sediments should be further explored (He et al., 2016). Nevertheless, by tracing the vertical evolution of DOM chemistry, a novel insight (e.g., increase of DOM recalcitrance with depth) into carbon sequestration and burial during the water-level rising period of TGR was noted in this work, which would help to better constrain the carbon budget in inland waters. Concerning the global blooming of reservoirs, the vertical evolution of DOM chemistry, which tightly links to carbon burial in reservoirs, should be further explored in multiple reservoirs from different climatic regions (Grill et al., 2019).

5. Conclusions

This research demonstrates the effect of reservoir construction on the vertical heterogeneity of DOM in a large and deep tributary of TGR during the water-level rising period. Significant variations in DOM chemistry including sources and composition among surface, middle and bottom water in vertical profile were revealed by a series of complementary techniques. Higher terrestrial signal with more biologically recalcitrant DOM and higher molecular weight in middle and bottom water than surface water was uncovered, which was mainly resulted from reservoir construction-induced physiochemical variations (e.g., density currents). Considering the various carbon cycling processes are involved, reservoir construction induced vertical heterogeneity of DOM likely contributes to the reducing of CO_2 emission and the enhancement of organic carbon burial during the water-level rising period. The mechanism of the vertical profile variation of DOM chemistry and its seasonal variability in reservoirs should be further explored for a better understanding of the interruptions of reservoir constructions on inland biogeochemical cycles.

Declaration of competing interest

The authors declare that they have no known competing financial interests that could have appeared to influence the work reported in this manuscript.

Acknowledgment

We acknowledge Prof. Rudolf Jaffé for his constructive suggestions and comments on an early version of this manuscript. This work is supported by the National Science Foundation of China [41773098 and 41973070 to D. He], the Qianjiang talent program [to D. He], and the hundred talent program of Zhejiang University [188020*194231701/008 and 188020-193810201/102 to D. He].

References

Amon, R.M.W., Rinehart, A.J., Duan, S., Louchouarn, P., Prokushkin, A., Guggenberger, G., Holmes, R. M. (2012). Dissolved organic matter sources in large Arctic rivers. Geochimica et Cosmochimica Acta, 94, 217-237.

Arstegui, J., Duarte, C.M., Agust, S., Doval, M., Álvarez-Salgado. X.A., Hansell, D.A. (2002). Dissolved organic carbon support of respiration in the dark ocean. Science, 298(5600), 1967-1967.

Bergauer, K., Fernandez-Guerra, A., Garcia, J.A.L., Sprenger, R.R., Stepanauskas, R., Pachiadaki, M.G., … Herndl, G.J. (2018). Organic matter processing by microbial communities throughout the Atlantic water column as revealed by metaproteomics. Proceedings of the National Academy of Sciences of the United States of America, 115(3), 201708779.

Burford, M.A., Green, S.K., Cook, A.J., Johnson, S.A., Kerr, J.G., O'Brien, K.R. (2012). Sources and fate of nutrients in a subtropical reservoir. Aquatic Sciences, 74(1), 179-190.

Butturini, A., Herzsprung, P., Lechtenfeld, O.J., Venturi, S., Amalfitano, S., Vazquez, E., … Fazi, S. (2020). Dissolved organic matter in a tropical saline-alkaline

lake of the East African Rift Valley. Water Research, 173, 115532.

Catalán, N., Casas-Ruiz, J.P., Von Schiller, D., Proia, L., Obrador, B., Zwirnmann, E., Marcé, R. (2017), Biodegradation kinetics of dissolved organic matter chromatographic fractions in an intermittent river, Journal of Geophysical Research: Biogeosciences, 122, 131-144.

Cawley, K.M., Butler, K.D., Aiken, G.R., Larsen, L.G., Huntington, T.G., Mcknight, D.M. (2012). Identifying fluorescent pulp mill effluent in the Gulf of Maine and its watershed. Marine Pollution Bulletin, 64(8), 1678-1687.

Chen, H., Stubbins, A., Perdue, E.M., Green, N.W., Helms, J.R., Mopper, K., Hatcher, P.G. (2014). Ultrahigh resolution mass spectrometric differentiation of dissolved organic matter isolated by coupled reverse osmosis-electrodialysis from various major oceanic water masses. Marine Chemistry, 164, 48-59.

Chen, Q., Shi, W., Huisman, J., Maberly, S.C., Zhang, J., Yu, J., … Yi, Q. (2020). Hydropower reservoirs on the upper Mekong River modify nutrient bioavailability downstream. National Science Review, 7(9), 1449-1457.

Cory, R.M., Harrold, K.H., Neilson, B.T., Kling, G.W. (2015). Controls on dissolved organic matter (DOM) degradation in a headwater stream: the influence of photochemical and hydrological conditions in determining light-limitation or substrate-limitation of photo-degradation. Biogeosciences, 12(22), 6669-6685.

Cory, R.M., Ward, C.P., Crump, B.C., Kling, G.W. (2014). Sunlight controls water column processing of carbon in arctic fresh waters. Science, 345(6199), 925-928.

Dai, Z., Liu, J.T. (2013). Impacts of large dams on downstream fluvial sedimentation: an example of the Three Gorges Dam (TGD) on the Changjiang (Yangtze River). Journal of Hydrology, 480, 10-18.

D'Andrilli, J., Cooper, W.T., Foreman, C.M., Marshall, A.G. (2015). An ultrahigh-resolution mass spectrometry index to estimate natural organic matter lability. Rapid Communications in Mass Spectrometry, 29(24), 2385-2401.

Dittmar, T., Koch, B., Hertkorn, N., Kattner, G. (2008). A simple and efficient method for the solid-phase extraction of dissolved organic matter (SPE-DOM) from seawater. Limnology and Oceanography Methods, 6(6), 230-235.

Fellman, J.B., Hood, E., Spencer, R.G.M. (2010). Fluorescence spectroscopy opens new windows into dissolved organic matter dynamics in freshwater ecosystems: A review. Limnology and Oceanography, 55(6), 2452-2462.

Findlay, S.E.G., Sinsabaugh, R.L., Sobczak, W.V., Hoostal, M. (2003). Metabolic and structural response of hyporheic microbial communities to variations in supply of dissolved organic matter. Limnology and Oceanography, 48(4), 1608-1617.

Gareis, J.A.L., Lesack, L.F.W., Bothwell, M.L. (2010). Attenuation of in situ UV radiation in Mackenzie Delta lakes with varying dissolved organic matter compositions. Water Resources Research, 46(9).

Gonsior, M., Zwartjes, M., Cooper, W.J., Song, W., Ishida, K. P., Tseng, L.Y., ⋯ Schmitt-Kopplin, P. (2011). Molecular characterization of effluent organic matter identified by ultrahigh resolution mass spectrometry. Water Research, 45(9), 2943-2953.

Graeber, D., Gelbrecht, J., Pusch, M.T., Anlanger, C., Schiller, D.V. (2012). Agriculture has changed the amount and composition of dissolved organic matter in Central European headwater streams. Science of the Total Environment, 438(3), 435-446.

Grill, G., Lehner, B., Thieme, M., Geenen, B., Tickner, D., Antonelli, F., ... Macedo, H.E. (2019). Mapping the world's free-flowing rivers. Nature, 569(7755), 215-221.

Hansen, A.M., Kraus, T.E., Pellerin, B.A., Fleck, J.A., Downing, B.D., Bergamaschi, B.A. (2016). Optical properties of dissolved organic matter (DOM): Effects of biological and photolytic degradation. Limnology and Oceanography, 61(3), 1015-1032.

Hertkorn, N., Benner, R., Frommberger, M., Schmitt-Kopplin, P., Witt, M., Kaiser, K., Kettrup, A., Hedges, J.I. (2006). Characterization of a major refractory component of marine dissolved organic matter. Geochimica et Cosmochimica Acta, 70(12), 2990-3010.

He, W., Chen, M., Schlautman, M.A., Hur, J. (2016). Dynamic exchanges between DOM and POM pools in coastal and inland aquatic ecosystems: a review. Science of the Total Environment, 551-552, 415-428.

He, C., Zhang, Y., Li, Y., Zhuo, X., Li, Y., Zhang, C., Shi, Q. (2020). In-House Standard Method for Molecular Characterization of Dissolved Organic Matter by FT-ICR Mass Spectrometry. ACS Omega, 5, 20, 11730-11736.

He, D., He, C., Li, P., Zhang, X., Shi, Q., Sun, Y. (2019). Optical and Molecular Signatures of Dissolved Organic Matter Reflect Anthropogenic Influence in a Coastal River, Northeast China. Journal of Environmental Qualty, 48, 603-613.

He, D., Wang, K., Pang, Y., He, C., Li, P., Li, Y., Xiao, S., Shi, Q., Sun, Y. (2020). Hydrological management constraints on the chemistry of dissolved organic matter in the Three Gorges Reservoir. Water Research, 187(15), 1-10.

He, X., Chen, Z., Li, F. (2018). A discussion about what's the better computing method for critical depth on The Three Gorges reservoir. Water Science and Engineering Technology, 2, 1-5.

Henderson, R.K., Baker, A., Parsons, S.A., Jefferson, B. (2008). Characterisation of algogenic organic matter extracted from cyanobacteria, green algae and diatoms. Water Research, 42(13), 3435-3445.

Hu, J., Yang, S.F., Wang, X. (2013). Sedimentation in Yangtze River above Three Gorges Project since 2003. Journal of Sediment Research, 1, 39-44.

Huguet, A., Vacher, L., Relexans, S., Saubusse, S., Froidefond, J.M., Parlanti, E. (2009). Properties of fluorescent dissolved organic matter in the Gironde Estuary. Organic Geochemistry, 40(6), 706-719.

Jacinthe, P.A., Filippelli, G.M., Tedesco, L.P., Raftis, R. (2012). Carbon storage and greenhouse gases emission from a fluvial reservoir in an agricultural landscape. Catena, 94(2), 53-63.

Jaffé, R., McKnight, D., Maie, N., Cory, R., McDowell, W.H., Campbell, J.L. (2008). Spatial and temporal variations in DOM composition in ecosystems: The importance of long-term monitoring of optical properties. Journal of Geophysical Research: Biogeosciences, 113(G4).

Jaffé, R., Yamashita, Y., Maie, N., Cooper, W.T., Dittmar, T., Dodds, W.K., et al. (2012). Dissolved organic matter in headwater streams: compositional variability across climatic regions of North America. Geochimica et Cosmochimica Acta, 94(4), 95-108.

Ji, D., Liu, D., Yang, Z., Xiao, S. (2010). Hydrodynamic characteristics of Xiangxi Bay in Three Gorges Reservoir. Science China, 40 (1), 101-112.

Jiao, N., Herndl, G.J., Hansell, D.A., Benner, R., Kattner, G., Wilhelm, S.W., … Chen, F. (2010). Microbial production of recalcitrant dissolved organic matter: long-term carbon storage in the global ocean. Nature Reviews Microbiology, 8(8), 593-599.

Kellerman, A.M., Guillemette, F., Podgorski, D.C., Aiken, G.R., Butler, K.D., Spencer, R.G. (2018). Unifying concepts linking dissolved organic matter composition to persistence in aquatic ecosystems. Environmental Science & Technology, 52(5), 2538-2548.

Kujawinski, E.B., Del Vecchio, R., Blough, N.V., Klein, G.C., Marshall, A.G. (2004). Probing molecular-level transformations of dissolved organic matter: insights on photochemical degradation and protozoan modification of DOM from electrospray ionization Fourier transform ion cyclotron resonance mass spectrometry. Marine Chemistry, 92(1-4), 23-37.

Lavonen, E.E., Kothawala, D.N., Tranvik, L.J., Gonsior, M., Schmitt-Kopplin, P., Kohler, S.J. (2015). Tracking changes in the optical properties and molecular composition of dissolved organic matter during drinking water production. Water Research, 85, 286-294.

Lawson, R., Anderson, M.A. (2007). Stratification and mixing in Lake Elsinore, California: an assessment of axial flow pumps for improving water quality in a shallow eutrophic lake. Water Research, 41(19), 4457-4467.

Lee, C., Wakeham, S.G. (1992). Organic matter in the water column: future research challenges. Marine Chemistry, 39, 95-118.

Li, P., Chen, L., Zhang, W., Huang, Q. (2015). Spatiotemporal distribution, sources, and photobleaching imprint of dissolved organic matter in the Yangtze Estuary and its adjacent sea using fluorescence and parallel factor analysis. Plos One, 10(6), 1-18.

Loginova, A.N., Thomsen, S., Engel, A. (2016). Chromophoric and fluorescent dissolved organic matter in and above the oxygen minimum zone off Peru. Journal of Geophysical Research, 121(11), 7973-7990.

Ly, Q.V., Maqbool, T., Hur, J. (2017). Unique characteristics of algal dissolved organic matter and their association with membrane fouling behavior: a review. Environmental Science and Pollution Research, 24(12), 11192-11205.

Maavara, T., Chen, Q., Meter, K.V., Brown, L.E., Zhang, J., Ni, J., Zarfl, C. (2020). River dam impacts on biogeochemical cycling. Nature Reviews Earth & Environment, 1(2), 103-116.

Maavara, T., Lauerwald, R., Regnier, P., Van Cappellen, P. (2017). Global perturbation of organic carbon cycling by river damming. Nature Communications, 8, 1-10.

Martin, J.L., McCutcheon, S.C. (1998). Hydrodynamics and Transport for Water Quality Modeling.

Medeiros, P.M., Seidel, M., Powers, L.C., Dittmar, T., Hansell, D.A., Miller, W.L. (2015a). Dissolved organic matter composition and photochemical transformations in the northern North Pacific Ocean. Geophysical Research Letters, 42(3), 863-870.

Medeiros, P.M., Seidel, M., Ward, N.D., Carpenter, E.J., Gomes, H.D., Niggemann, J., ... Dittmar, T. (2015b). Fate of the Amazon River dissolved organic matter in the tropical Atlantic Ocean. Global Biogeochemical Cycles. 29 (5), 677-690.

Melendez-Perez, J.J., Martínez-Mejía, M.J., Awan, A.T., Fadini, P.S., Mozeto, A.A., Eberlin, M.N. (2016). Characterization and comparison of riverine, lacustrine, marine and estuarine dissolved organic matter by ultra-high resolution and accuracy Fourier transform mass spectrometry. Organic Geochemistry, 101, 99-107.

Mendonça, R., Kosten, S., Sobek, S., Cardoso, S.J., Figueiredo-Barros, M.P., Estrada, C.H.D., Roland, F. (2016). Organic carbon burial efficiency in a subtropical hydroelectric reservoir. Biogeosciences, 13(11), 3331-3342.

Mendonça, R., Müller, R.A., Clow, D., Verpoorter, C., Raymond, P., Tranvik, L.J., Sobek, S. (2017). Organic carbon burial in global lakes and reservoirs. Nature Communications, 8(1), 1694-1694.

Miller, M.P., McKnight, D.M., Chapra, S.C., Williams, M.W. (2009). A model of degradation and production of three pools of dissolved organic matter in an alpine lake. Limnology and Oceanography, 54(6), 2213-2227.

Murphy, K.R., Bro, R., Stedmon, C.A. (2014). Chemometric analysis of organic matter fluorescence. Aquatic Organic Matter Fluorescence, 261(1), 339-375.

Murphy, K.R., Hambly, A., Singh, S., Henderson, R.K., Baker, A., Stuetz, R., et al. (2011). Organic matter fluorescence in municipal water recycling schemes: toward a unified PARAFAC model. Environmental Science and Technology, 45(7), 2909-2916.

Murphy, K.R., Ruiz, G.M., Dunsmuir, W.T., Waite, T.D. (2006). Optimized parameters for fluorescence-based verification of ballast water exchange by ships. Environmental Science and Technology, 40(7), 2357-2362.

Ohno, T., Chorover, J., Omoike, A., Hunt, J. (2007). Molecular weight and humification index as predictors of adsorption for plant- and manure-derived dissolved organic matter to goethite. European Journal of Soil Science, 58(1), 125-132.

Osburn, C.L., Handsel, L.T., Peierls, B.L., Paerl, H.W. (2016). Predicting sources of dissolved organic nitrogen to an estuary from an agro-urban coastal watershed. Environmental Science and Technology, 50(16), 1-17.

Osburn, C.L., Wigdahl, C.R., Fritz, S.C., Saros, J.E. (2011). Dissolved organic matter composition and photoreactivity in prairie lakes of the U.S. Great Plains. Limnology and Oceanography, 56(6), 2371-2390.

Padisák, J., Barbosa, F.A.R., Koschel, R., Krienitz, L. (2003). Deep layer cyanoprokaryota maxima in temperate and tropical lakes. Ergebnisse Der Limnologie, 175-199.

Raymond, P.A., Bauer, J.E. (2001). Riverine export of aged terrestrial organic matter to the North Atlantic Ocean. Nature, 409(6819), 497-500.

Saadi, I., Borisover, M., Armon, R., Laor, Y. (2006). Monitoring of effluent DOM biodegradation using fluorescence, UV and DOC measurements. Chemosphere, 63(3), 530-539.

Schmidt, F., Elvert, M., Koch, B.P., Witt, M., Hinrichs, K.U. (2009). Molecular characterization of dissolved organic matter in pore water of continental shelf sediments. Geochimica et Cosmochimica Acta, 73(11), 3337-3358.

Seidel, M., Yager, P.L., Ward, N.D., Carpenter, E.J., Gomes, H.R., Krusche, A.V., ... Medeiros, P.M. (2015). Molecular-level changes of dissolved organic matter along the Amazon River-to-ocean continuum. Marine Chemistry, 177, 218-231.

She, Z., Wang, J., He, C., Pan, X., Li, Y., Zhang, S., Shi, Q., Yue, Z. (2021). The stratified distribution of dissolved organic matter in an AMD lake revealed by multi-sample evaluation procedure. Environmental Science & Technology, doi: 10.1021/acs.est.0c05319.

Stedmon, C.A., Markager, S. (2005). Resolving the variability in dissolved organic matter fluorescence in a temperate estuary and its catchment using PARAFAC analysis. Limnology and Oceanography, 50(2), 686-697.

Stedmon, C.A., Markager, S., Bro, R. (2003). Tracing dissolved organic matter in aquatic environments using a new approach to fluorescence spectroscopy. Marine Chemistry, 82(3), 239-254.

Stedmon, C.A., Bro, R. (2008). Characterizing dissolved organic matter fluorescence with parallel factor analysis: a tutorial. Limnology and Oceanography Methods, 6(11), 572-579.

Stubbins, A., Spencer, R.G.M., Chen, H., Hatcher, P.G., Mopper, K., Hernes, P.J., … Six, J. (2010). Illuminated darkness: molecular signatures of Congo River dissolved organic matter and its photochemical alteration as revealed by ultrahigh precision mass spectrometry. Limnology and Oceanography, 55(4), 1467-1477.

Stubbins, A., Lapierre, J.-F., Berggren, M., Prairie, Y.T., Dittmar, T., Giorgio, P.A. del. (2014). What's in an EEM? Molecular Signatures Associated with Dissolved Organic Fluorescence in Boreal Canada. Environmental Science & Technology, 48(18), 10598-10606.

Wang, F. (2020). Impact of a large sub-tropical reservoir on the cycling of nutrients in a river. Water Research, 186, 116363.

Wang, K., Pang, Y., Gao, C., Chen, L., Jiang, X., Li, P., … He, D. (2021a). Hydrological management affected dissolved organic matter chemistry and organic carbon burial in the Three Gorges Reservoir. Water Research, 199, 117195-117195.

Wang, K., Pang, Y., He, C., Li, P., Xiao, S., Sun, Y., Zhang, Y., Shi, Q., He, D. (2019). Optical and Molecular Signatures of Dissolved Organic Matter in Xiangxi Bay and Mainstream of Three Gorges Reservoir, China: Spatial Variations and Environmental Implications, Science of the Total Environment, 657, 1274-1284.

Wang, K., Pang, Y., Li, Y., He, C., Shi, Q., Wang, Y., He, D. (2021b). Characterizing Dissolved Organic Matter Across a Riparian Soil-Water Interface: Preliminary Insights from a Molecular Level Perspective. ACS Earth and Space Chemistry.

Yamashita, Y., Panton, A., Mahaffey, C., Jaffé, R. (2011). Assessing the spatial and temporal variability of dissolved organic matter in Liverpool Bay using excitation-emission matrix fluorescence and parallel factor analysis. Ocean Dynamics, 61(5), 569-579.

Yang, F., Yang, Z., Ji D., Su, Q., Long, L., Liu, X., Wang, Y., Zhao, C. (2019). Spatial distribution characteristics of Chlorophyll-a and nutrient salts in tributaries of different river sections in the Three Gorges Reservoir area during the flood season. Environmental Science, 40(11), 4944-4952.

Yang, L., Liu, D. F., Yang, Z.J., Yuan, L.I., Zhang, P. (2015). Density-stratified flow of Xiangxi Bay at Three Gorges Reservoir based on the tracer principle of inorganic ion. Resources and Environment in the Yangtze Basin, 24(2), 278-285.

Yang, Z., Cheng, B., Xu, Y., Liu, D., Ma, J., Ji, D. (2018). Stable isotopes in water indicate sources of nutrients that drive algal blooms in the tributary bay of a subtropical reservoir. Science of The Total Environment, 634, 205–213.

Yi, Y., Zhong, J., Bao, H., Mostofa, K.M.G., Xu, S., Xiao, H., Li, S. (2021). The impacts of reservoirs on the sources and transport of riverine organic carbon in the karst area: A multi-tracer study. Water Research, 194, 116933-116933.

Zhang, Q., Song, L., Ji D., Fang, H., He, J., Huo, J., Liu, X., Wang, Y., Zhu, X. (2019). Relationship between water quality of Xiangxi River Reservoir and the algal blooms in non-return area in the Three Gorges Reservoir Area. China Environmental Science, 39(7), 3018-3026.

Zhou, S., Shao, Y., Gao, N., Deng, Y., Li, L., Deng, J., Tan, C. (2014). Characterization of algal organic matters of Microcystis aeruginosa: biodegradability, DBP formation and membrane fouling potential. Water Research, 52, 199-207.

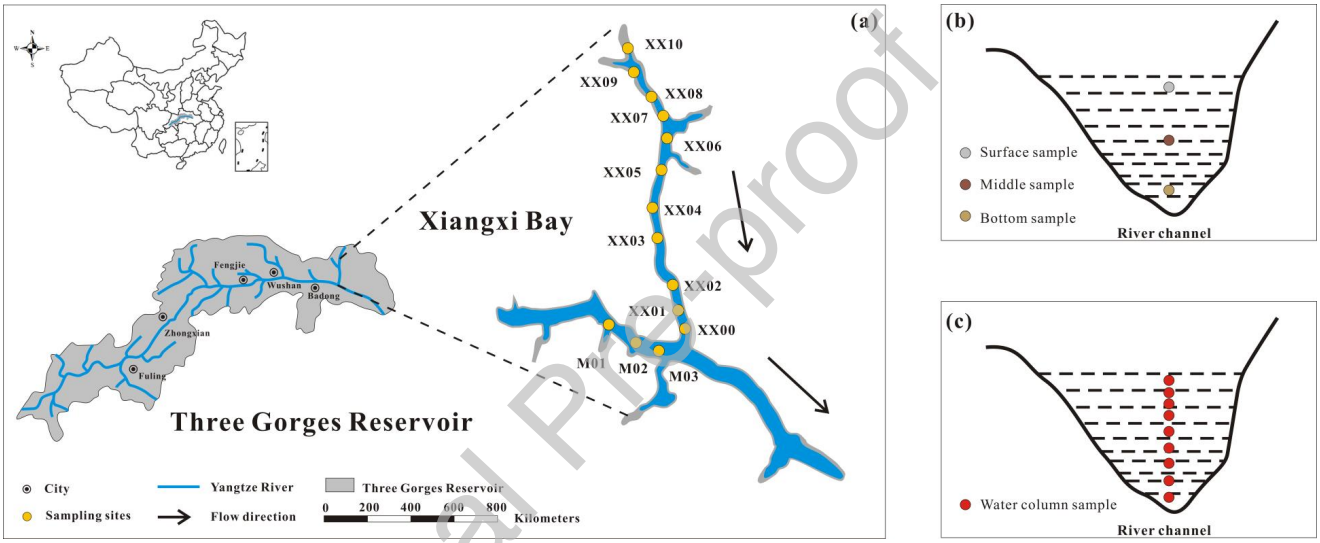

Fig. 1 Study area and sampling sites. Sampling sites were selected along the upstream to downstream transect (XX10 to XX00) and mainstream (M01 to M03) (a); Surface, middle, and bottom samples were collected (b); High resolution water column samples in XX00 (sampling in depth of 2m, 5m, 10m, 15m, 20m, 30m, 40m, 50m, 60m) were collected (c).

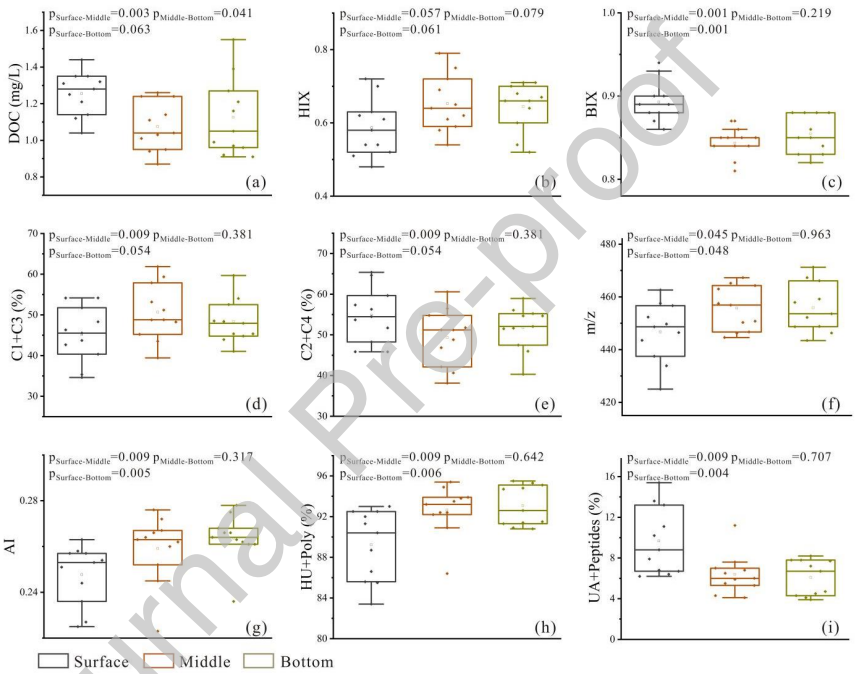

Fig. 2 Property variation of DOM between surface, middle, and bottom water: (a) DOC, (b) HIX, (c) BIX, (d) C1+C3, (e) C2+C4, (f) m/z, (g) AI, (h) HU+Poly, (i) UA+Peptides. HU: Highly unsaturated compounds; Poly: Polyphenols; UA: Unsaturated aliphatics. The box symbol denotes the mean value of the dataset including surface and bottom samples, with the horizontal lines in the box denoting the 25th, 50th, and 75th percentile values.

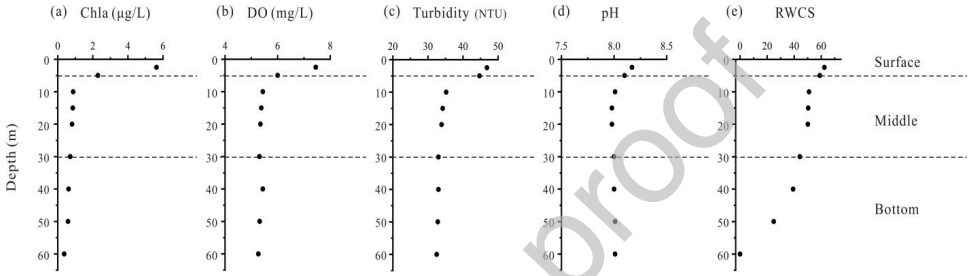

Fig. 3 Vertical profiles of physiochemical parameters. Two horizontal dashed lines divide XXB into three layers: surface (0-5 m), middle (5-30 m), and bottom (30−60 m). (a) Chla: $R^2_{surface\text{-}bottom}$=0.41, $R^2_{middle\text{-}bottom}$=0.91; (b) DO: $R^2_{surface\text{-}bottom}$=0.36, $R^2_{middle\text{-}bottom}$=0.38; (c) Turbidity: $R^2_{surface\text{-}bottom}$=0.47, $R^2_{middle\text{-}bottom}$=0.82; (d) pH: $R^2_{surface\text{-}bottom}$=0.26, $R^2_{middle\text{-}bottom}$=0.29; (e) RWCS: $R^2_{surface\text{-}bottom}$=0.87, $R^2_{middle\text{-}bottom}$=0.81.

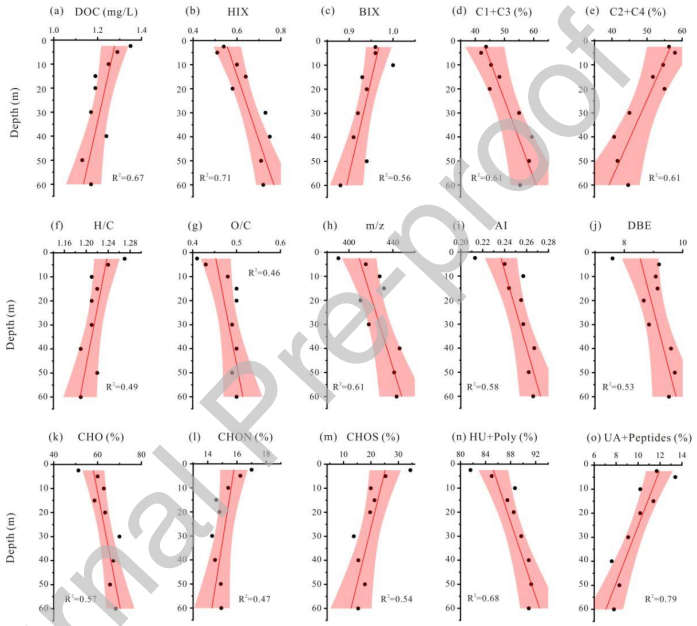

Fig. 4 Variation of DOM along vertical profile. (a) DOC, (b) HIX, (c) BIX, (d) C1+C3, (e) C2+C4, (f) H/C, (g) O/C, (h) m/z, (i) AI, (j) DBE, (k) CHO, (l) CHON, (m) CHOS, (n) HU+Poly, (o) UA+ Peptides. HU: Highly unsaturated compounds; Poly: Polyphenols; UA: Unsaturated aliphatics. Shaded area of red color indicates 95% confidence interval.

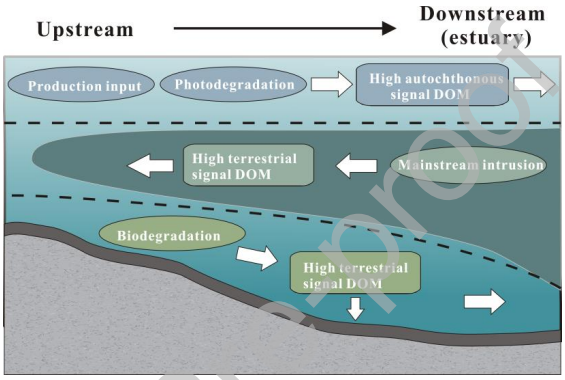

Fig. 5 Conceptual model of DOM variation in vertical profile of reservoir

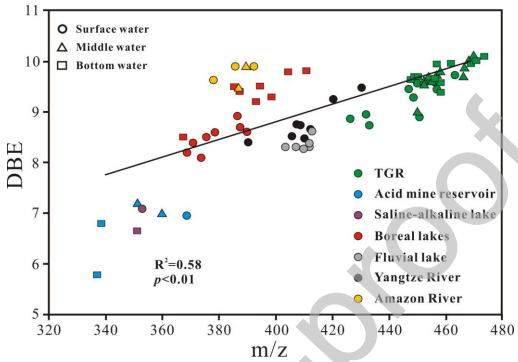

Fig. 6 Plot of m/z versus DBE of DOM from inland ecosystems including TGR (this study), acid mine reservoir (She et al., 2021), saline-alkaline lake (Butturini et al., 2020), boreal lakes (Valle et al., 2020), fluvial lake (Liu et al., 2020), Yangtze River (Pang et al., 2020), and Amazon River (Seidel et al., 2015).